Geochemistry, Geophysics, Geosystems

RESEARCH ARTICLE
10.1029/2019GC008694

Key Points:
- Mg in acid-sulfate fluids is seawater derived
- Li isotopes in acid-sulfate fluids trace basement alteration

Supporting Information:
- Supporting Information S1

Correspondence to:
F. K. Wilckens,
fwilckens@marum.de

Citation:
Wilckens, F. K., Reeves, E. P., Bach, W., Seewald, J. S., & Kasemann, S. A. (2019). Application of B, Mg, Li, and Sr isotopes in acid-sulfate vent fluids and volcanic rocks as tracers for fluid-rock interaction in back-arc hydrothermal systems. *Geochemistry, Geophysics, Geosystems*, *20*, 5849–5866. https://doi.org/10.1029/2019GC008694

Received 9 SEP 2019
Accepted 5 NOV 2019
Accepted article online 15 NOV 2019
Published online 6 DEC 2019

Application of B, Mg, Li, and Sr Isotopes in Acid-Sulfate Vent Fluids and Volcanic Rocks as Tracers for Fluid-Rock Interaction in Back-Arc Hydrothermal Systems

Frederike K. Wilckens[1], Eoghan P. Reeves[1,2,3], Wolfgang Bach[1], Jeffrey S. Seewald[2], and Simone A. Kasemann[1]

[1]MARUM—Center for Marine Environmental Sciences and Faculty of Geosciences University of Bremen, Bremen, Germany, [2]Department of Marine Chemistry and Geochemistry, Woods Hole Oceanographic Institution, Woods Hole, MA, USA, [3]Department of Earth Science and K.G. Jebsen Centre for Deep Sea Research, University of Bergen, Bergen, Norway

Abstract The Manus Basin hosts a broad range of vent fluid compositions typical for arc and back-arc settings, ranging from black smoker to acid-sulfate styles of fluid venting, as well as novel intermediate temperature and composition "hybrid" smokers. We investigated B, Li, Mg, and Sr concentrations and isotopic compositions of these different fluid types as well as of fresh and altered rocks from the same study area to understand what controls their compositional variability. In particular, the formation of acid-sulfate and hybrid smoker fluids is still poorly understood, and their high Mg concentrations are explained either by dissolution of Mg-bearing minerals in the basement or by mixing between unmodified seawater and magmatic fluids. Mg isotope ratios of the acid-sulfate fluids from the Manus Basin are seawater-like, which supports the idea that acid-sulfate fluids in this study area predominantly form by mixing between unmodified seawater and a Mg-free magmatic fluid. Changes in the B, Li, and Sr isotope ratios relative to seawater indicate water-rock interaction in all acid-sulfate fluids. Further, the combination of δ^7Li with B concentrations of the same fluids links changes in δ^7Li to changes in (1) basement alteration, (2) water-to-rock ratios during water-rock interaction, and/or (3) the reaction temperature. These isotope systems, thus, allow tracing of basement composition and acid-sulfate-driven alteration of the back-arc crust and help increase our understanding of hydrothermal fluid-rock interactions and the behavior of fluid-mobile elements.

1. Introduction

Hydrothermal vent fluids in submarine arc and back-arc environments are influenced by the complex interplay between mantle wedge, subducting slab, seafloor morphology, and volcanic activity. In consequence, fluids venting in these tectonic settings are characterized by a broad range of chemical and physical variability (Araoka et al., 2016; Gamo et al., 1997; Gena et al., 2006; Reeves et al., 2011; Resing et al., 2007; Seewald et al., 2015; Wilckens et al., 2018; Yamaoka et al., 2015). A unique type of vent fluid, which is known from several arc and back-arc sites in the Western Pacific, are acid-sulfate fluids. Acid-sulfate fluids are characterized by low pH, high Mg and sulfate concentrations, and high gas contents (Gamo et al., 1997; Lupton et al., 2006., 2011; Resing et al., 2007; de Ronde et al., 2011; Butterfield et al., 2011; Seewald et al., 2015). As a result of their distinct chemical composition compared with other hydrothermal fluids, the fluids may have a profound influence on the global hydrothermal fluxes of, for example, aluminum or carbon dioxide (CO_2) (Butterfield et al., 2011; Lupton et al., 2006).

The formation of acid-sulfate fluids differs from that of black smoker fluids (Figure 1). Black smoker fluids form mainly through water-rock interaction of seawater delivered to the subsurface via hydrothermal convection (Figure 1a). During water-rock interaction as temperatures increase beyond 150 °C, Mg and sulfate are depleted in the fluids due to precipitation of anhydrite ($CaSO_4$) and incorporation of Mg into secondary Mg-OH silicates (Butterfield, 1999; James et al., 2003; Seyfried, 1987) (process 1 in Figure 1a). Fluid chemistry is further modified by dissolution of minerals and leaching of metals, alkali, and alkaline elements at high temperatures, phase separation, and addition of magmatic fluids (2 and 3 in Figure 1a).

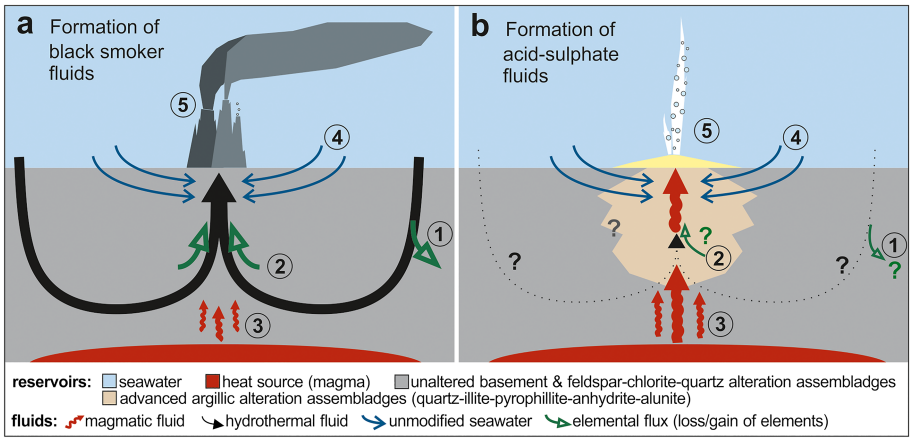

Figure 1. Sketch illustrating the formation of (a) black smoker fluids and (b) acid-sulfate fluids. The thickness of the arrows is equal to the flux intensity. The numbers indicate the processes or sources that influence the fluid chemistry: (1) deep subsurface convective circulation of seawater and loss of Mg, SO_4 during formation of Mg-hydroxysilicates, and anhydrite at elevated temperatures; (2) dissolution of minerals and leaching of elements during high-temperature water-rock interactions and phase separation; (3) magmatic fluid degassing; (4) entrainment of unmodified seawater in the shallow subsurface; and (5) venting at the seafloor and precipitation of minerals.

In contrast, the formation of acid-sulfate fluids does not involve a significant hydrothermal circulation cell or a primary seawater source fluid (Figure 1b). Instead, magmatic H_2O-CO_2-SO_2-HCl fluids (Figure 1b, red arrows) discharge to the seafloor, mixing with relatively unmodified seawater during upflow (Seewald et al., 2015). This general scenario can explain the exceptionally low pH, high Mg and SO_4 concentrations, and seawater-like Sr isotope compositions of acid-sulfate fluids (Seewald et al., 2015). Previous studies examining the formation of acid-sulfate fluids invoke water-dominated water-rock interaction with a highly altered crust based on the limited enrichments of fluid mobile elements (e.g., Li, Cs, and Rb) in acid-sulfate fluids relative to seawater (Gamo et al., 1997; Gena et al., 2006; Seewald et al., 2015). However, conditions during the interaction of magmatic fluid, evolved seawater, and basement rock within magmatic hydrothermal systems in arc and back-arc environments are poorly understood.

To improve our understanding of the formation of acid-sulfate fluids and associated crustal alteration, we report aqueous lithium (Li), boron (B), magnesium (Mg), and strontium (Sr) isotope ratios in a range of

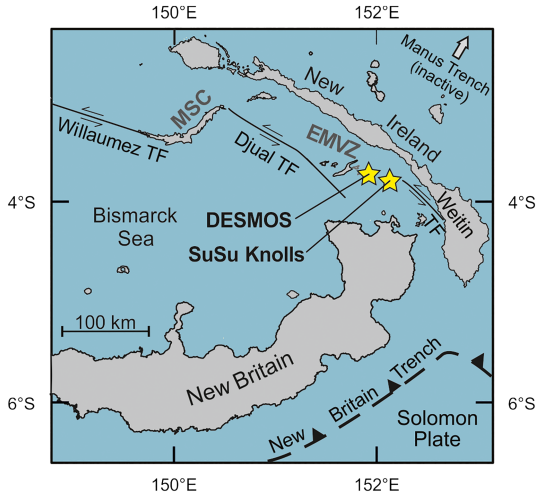

Figure 2. Tectonic setting of the Manus Basin. Yellow stars indicate the sample locations within the EMVZ. Major tectonic plates and the plate motions are indicated with black and gray arrows (map after Tivey et al., 2006). MSC = Manus Spreading Center; EMVZ = Eastern Manus Volcanic Zone; TF = tsransform fault.

acid-sulfate and black smoker fluids from the Manus Basin, Bismarck Sea, Papua New Guinea (Fig. 2). The Manus back-arc basin hosts a range of hydrothermal systems (Craddock et al., 2010; Gamo et al., 1997; Reeves et al., 2011; Seewald et al., 2015, 2019) and is well suited to assess the broad range of physical and chemical processes that regulate vent fluid composition. The compositional variability in the vent fluids is a result of phase separation processes, the heterogeneous composition of the basement (from basaltic andesite to rhyodacite), and variable inputs of magmatic fluids into the hydrothermal circulation cell (Gamo et al., 1997; Reeves et al., 2011; Seewald et al., 2015). The high-temperature (high-T) fluids venting at the Manus Spreading Center are similar to black smoker fluids at mid-ocean ridge settings, reflecting the more mid-ocean ridge basalt (MORB)-like composition of the oceanic crust (Reeves et al., 2011; Seewald et al., 2019; Wilckens et al., 2018; Yamaoka et al., 2015). In contrast, vent fluids from the Eastern Manus Volcanic Zone (EMVZ) have a compositional range from high-temperature (high-T) and low-temperature (low-T) fluids with variable gas concentrations to acid-sulfate fluids and hybrid forms of acid-sulfate and smoker-type fluids. Particularly, North Su volcano within the EMVZ hosts some of the most highly acidic acid-sulfate-type fluids discovered to date with pH <1 and SO_4 concentrations >150 mM (Seewald et al., 2015). Mg isotope data allow us to test whether Mg in acid-sulfate fluids is derived from seawater or leached from the oceanic crust. The application of Li, B, and Sr isotopes in acid-sulfate fluids provides a promising tool for understanding magmatic-hydrothermal water-rock interaction and for tracking the progressive alteration of the oceanic crust during interaction with acid-sulfate fluids.

2. Study Area

2.1. Tectonic Setting

The Manus Basin is located in the northeastern Bismarck Sea, Papua New Guinea, and is bordered by the inactive Manus Trench in the northeast, the Willaumez Rise in the northwest, and the New Britain Trench in the south (Lee & Ruellan, 2006; Taylor et al., 1994) (Figure 2). The basin is a rapidly opening back-arc basin, which formed during the northward subduction of the Solomon plate along the New Britain Trench. The acid-sulfate fluids are located in the EMVZ, between the Djaul and Weitin transform faults. Volcanic rock types in this area range from basaltic andesites to dacites. The chemical composition of these rocks resembles that of island arc basalts (Kamenetsky et al., 2001; Sinton et al., 2003; Pearce & Stern, 2006; Park et al., 2010; Beier et al., 2015). Hydrothermal activity occurs at several vent sites in the EMVZ (Craddock et al., 2010; Gamo et al., 1997; Reeves et al., 2011; Seewald et al., 2015, 2019). However, known areas of acid-sulfate venting are limited to the DESMOS caldera and at North Su within the SuSu Knolls neovolcanic edifice complex (Figure 2).

2.2. Hydrothermal Vent Sites

2.2.1. North Su

North Su is one of the volcanic edifices within SuSu Knolls, which overlie the andesitic Tumai Ridge. The hydrothermal fluids at the North Su hydrothermal field have a broad compositional range from high-T black smoker over diffuse to acid-sulfate fluids (Seewald et al., 2015, 2019). Black smoker fluids vent in the summit area and to the west of North Su, with temperatures up to 332 °C and pH between 2.8 and 4.8 (measured at 25 °C). Expansive fields of hybrid and white smokers and, in particular, acid-sulfate fluids vent south of the summit area. These acid-sulfate fluids mostly vent milky white smoke (likely elemental sulfur) with variable exit temperatures between 48 and 241 °C and pH between 0.87 and 1.9 (Bach et al., 2011; Reeves et al., 2015; Seewald et al., 2015).

2.2.2. DESMOS caldera

DESMOS caldera is also located in the EMVZ and describes a neovolcanic edifice north of SuSu Knolls, which rises to about 1,810-m depth. DESMOS has a caldera with a depression of 150 to 250 m, a width of about 1.5 to 2 km, and negligible sediment cover. Compared to North Su, DESMOS has more limited areas of hydrothermal activity, with white smoke venting only at a small poorly focused vent area 30 m in diameter. The so-called Onsen site venting on a ledge of the northern caldera wall emits acid-sulfate fluids (Gamo et al., 1997). Similar to North Su, the fluids are characterized by low exit temperatures of 69 to 117 °C and low pH from 0.95 to 1.4 (Seewald et al., 2015).

3. Methods

3.1. Sampling and Analytical Methods

Vent fluid samples (Table 1) were collected during the July–August 2006 MAGELLAN-06 expedition aboard the R/V *Melville* and a second SO-216 (BAMBUS) expedition aboard the R/V *Sonne* in June–July 2011. During MAGELLAN-06, vent fluids were sampled with isobaric gas-tight (IGT) fluid samplers (Seewald et al., 2002) and syringe-style "major" samplers deployed from the ROV *Jason II*. Sampling methods and locations from the 2006 campaign have been previously described (Craddock et al., 2010; Reeves et al., 2011; Seewald et al., 2015, 2019). During SO-216, vent fluid sampling was done with IGT fluid samplers as well as the "KIPS" (Kiel Pumping System) (Garbe-Schönberg et al., 2006) fluid pumping system deployed from ROV *MARUM-QUEST* (Bach et al., 2011). Typically, two IGT samples were taken at each orifice, but in some instances, collection of only one fluid sample was possible. Real-time measurements of temperature were taken during IGT sample collection, and reported temperatures represent the maximum measured value. Shipboard analysis of pH and processing of fluids was identical to that of the 2006 cruise (e.g., Reeves et al., 2011; Seewald et al., 2015). Fluid aliquots for major and trace element analyses were acidified to pH <2 with trace metal grade nitric acid, and subsamples of these aliquots were diluted 100-fold for measurement of aqueous SiO_2. For analyses of SO_4 concentrations, separate fluid aliquots were purged with N_2 to remove H_2S prior to storage. Typical uncertainties were ±0.02 pH units (2*SD*; Reeves et al., 2011; Seewald et al., 2015). The concentrations of Mg, Sr, aqueous SiO_2, Cl, and SO_4 in the fluids sampled in 2006 have been published previously (Craddock et al., 2010; Reeves et al., 2011; Seewald et al., 2015, 2019).

Mg concentrations were determined by ion chromatography (at Woods Hole Oceanographic Institution, samples of 2006) and inductively coupled plasma-optical emission spectrometry (ICP-OES; at University of Bremen, samples of 2011) onshore (Reeves et al., 2015; Seewald et al., 2015). Sr and Li concentrations in the acidified 2006 fluid samples were determined by inductively coupled plasma-mass spectrometry (ICP-MS) at Woods Hole Oceanographic Institution, and SiO_2 concentrations were determined by ICP-OES at the University of South Florida. Sr, Li, and SiO_2 concentrations in the 2011 fluid samples were determined by ICP-OES, while Cl and SO_4 were determined by ion chromatography (Uni. Bremen). Analytical uncertainties (2*RSD*) are ±10% for Li and Sr, ±5% for Cl and SO_4, ±3% for Mg, ±2% for SiO_2, and ±0.02 pH units.

Volcanic rock samples were collected during the MAGELLAN-06 expedition from DESMOS and SuSu Knolls using the ROV *Jason II*. Beier et al. (2015) described sample locations, sample preparation, and the petrology for the fresh volcanic rocks, and Wilckens et al. (2018) discussed the altered rock samples. Sr and Li contents for the volcanic rocks and two reference materials (basalt BM and granite GM) were analyzed by ICP-MS on a ThermoFinnigan Element2 at the Helmholtz-Zentrum Potsdam (GeoForschungsZentrum Potsdam) and at the Institute of Geosciences, University of Bremen, respectively. Sr and Li concentrations of the reference materials are within analytical uncertainty (<5%, 2*SD*) with literature values (Beier et al., 2015). For more details, see Beier et al. (2015) and Wilckens et al. (2018).

3.2. Sample Preparation and Isotope Ratio Measurements

The analytical procedures and measurements of Li, Sr, and Mg isotope ratios were performed in the Isotope Geochemistry Laboratory at MARUM—Centre for Marine Environmental Sciences, University of Bremen (Germany). Before isotope analysis, the volcanic rock samples were pulverized and digested using a mixture of concentrated, ultrapure HNO_3, HCl, and HF (hydrofluoric acid). Vent fluids were evaporated to dryness. Mg, Li, and Sr were separated from their sample matrix using specific separation methods outlined here.

For Sr isotope analysis about 300-ng Sr was loaded onto chromatograhic separation columns. The separation of Sr was done with Sr spec resin (modified after Pin & Bassin, 1992), and the separated Sr fraction was loaded together with a tantalum emitter onto rhenium filaments and measured with a ThermoFisher Scientific TRITON Plus thermal ionization mass spectrometer in dynamic mode. Strontium isotopic ratios are given as $^{87}Sr/^{86}Sr$ and were normalized to the stable $^{86}Sr/^{88}Sr$ of 0.1194 to correct for instrumental mass fractionation. The instrumental accuracy for $^{87}Sr/^{86}Sr$ was obtained by repeated analysis of the standard reference material NIST SRM 987, which gave a value of 0.710248 ± 0.000015 ($2SD_{mean}$, $n = 12$) that is in agreement with the published values analyzed by thermal ionization mass spectrometer (0.710250 ±

Table 1
Measured Concentrations of Boron, Lithium, Strontium, and Magnesium, Together With Isotope Data for Acid-Sulfate and Black Smoker Fluids From North Su and DESMOS and Previously Reported Data for the Same Vent Fluids

Edifice		Working ID	Year of sampling	IGT T[a]	pH[a]	Mg[a]	B[b]	Li	Sr[a]	Cl[a]	SO_4[a]	SiO_2[a]
				°C	25 °C	(mmol/kg)	(μmol/kg)	(μmol/kg)	(μmol/kg)	(mmol/kg)	(mmol/kg)	(mmol/kg)
Acid-sulfate (white smoker) fluids												
North Su	NS1	J2-221-IGT7	2006	48	1.8	49.6	505	35	86	520	37	3.7
	NS1	J2-221-IGT8	2006	47	1.9	50.4	484	30	85	527	35	3.0
	NS1	J2-221-M4	2006		1.9	49.8	464	34	87	524	—	3.3
	NS2	J2-221-IGT6	2006	206	0.9	39.2	797	27	58	443	132	9.9
	NS2	J2-221-IGT5	2006	215	0.9	41.1	718	34	64	456	120	8.6
	NS2	J2-221-M2	2006		0.9	41.1	704	34	63	457	—	8.9
	NS9	023-ROV-01	2011	95	1.4	44.7	465	37	66.0	477	61	4.4
	NS9	023-ROV-02	2011	103	1.2	42.7	472	41	59.3	456	72	5.8
DESMOS	D1	J2-220-IGT1	2006	113	1.0	44.9	474	24	71	492	147	8.3
	D1	J2-220-IGT2	2006	117	1.0	45.1	471	25	72	495	139	7.9
	D1	J2-220-M4	2006		1.3	50.0	446	29	86	n.d.	80	3.5
	D2	J2-220-IGT3	2006	69	1.4	49.2	471	21	79	502	59	5.7
	D2	J2-220-M2	2006		1.4	49.4	473	25	80	501	62	5.7
	D2	J2-220-IGT4	2006	70	1.4	49.3	487	31	78	n.d.	63	5.7
Hybrid smoker fluids												
North Su	NS4	J2-223-IGT5	2006	241	1.5	23.5	1,047	419	73	562	28	16.1
	NS4	J2-223-IGT6	2006	203	1.5	24.2	1,057	380	75	562	26	15.8
	NS8	021-ROV-01	2011	169	2.4	43.5	626	122	95	555	27	3.1
	NS11	047-ROV-03	2011	149	2.0	44.2	570	130	95	553	30	5.0
	NS11	047-ROV-04	2011	129	1.9	40.8	662	164	100	553	31	6.5
Black smoker fluids												
North Su	NS3	J2-223-IGT7	2006	300	3.5	3.4	1,416	806	232	665	1.6	16.7
	NS5	J2-227-IGT2	2006	299	3.4	7.4	1,073	562	215	550	0.9	14.9
	NS5	J2-227-M2	2006		4.8	27.4	934	348	151	544	—	—
	NS6	J2-227-IGT3	2006	325	2.8	1.6	1,740	833	410	773	0.7	16.0
	NS6	J2-227-M4	2006		2.9	5.1	1,555	766	367	668	-	—
	NS7	019-ROV-01	2011	332	3.2	15.3	1,298	581	297	662	9.9	—
	NS10	045-ROV-02	2011	312	4.8	18.9	1,356	500	199	662	—	14.9
Bottom SW		J2-228-M4	2006	3	7.9	52.4	419	28	91	540	28.2	0.13

Edifice		Working ID	Year of sampling	$\delta^{11}B$[b]	±	2SD	$\delta^{7}Li$	±	2SD	$^{87}Sr/^{86}Sr$[a]	±	2se	$\delta^{26}Mg$	±	2SD
				(‰)			(‰)						(‰)		
acid-sulfate (white smoker) fluids															
North Su	NS1	J2-221-IGT7	2006	35.0	±	0.1	23.1	±	0.1	0.70899	±	0.00001	-0.82	±	0.02
	NS1	J2-221-IGT8	2006	36.0	±	0.1	24.3	±	0.1	0.70895	±	0.00001	-0.91	±	0.03
	NS1	J2-221-M4	2006	36.0	±	0.1	23.8	±	0.2	0.70902	±	0.00001	-0.92	±	0.01
	NS2	J2-221-IGT6	2006	23.3	±	0.1	20.6	±	0.1	0.70870	±	0.00001	-0.83	±	0.04
	NS2	J2-221-IGT5	2006	24.8	±	0.2	22.0	±	0.0	-			-0.83	±	0.03
	NS2	J2-221-M2	2006	24.9	±	0.1	21.7	±	0.1	0.70885	±	0.00001	-0.86	±	0.04
	NS9	023-ROV-01	2011	33.0	±	0.2	19.2	±	0.3	0.70890	±	0.00001	-0.90	±	0.02
	NS9	023-ROV-02	2011	31.4	±	0.1	17.2	±	0.2	0.70876	±	0.00001	-0.86	±	0.02
DESMOS	D1	J2-220-IGT1	2006	35.3	±	0.1	29.2	±	0.1	0.70880	±	0.00001	-0.85	±	0.05
	D1	J2-220-IGT2	2006	35.0	±	0.1	29.3	±	0.1	0.70896	±	0.00001	-0.83	±	0.06
	D1	J2-220-M4	2006	38.6	±	0.1	29.8	±	0.1	0.70896	±	0.00001	-0.90	±	0.01
	D2	J2-220-IGT3	2006	36.0	±	0.1	29.7	±	0.1	0.70888	±	0.00001	-0.86	±	0.01
	D2	J2-220-M2	2006	35.8	±	0.1	29.5	±	0.1	0.70886	±	0.00001	-0.90	±	0.03
	D2	J2-220-IGT4	2006	35.8	±	0.1	30.1	±	0.2	0.70886	±	0.00001	-0.89	±	0.02
hybrid smoker fluids															
North Su	NS4	J2-223-IGT5	2006	20.7	±	0.1	6.2	±	0.1	0.70739	±	0.00000	-0.89	±	0.03
	NS4	J2-223-IGT6	2006	20.7	±	0.0	6.5	±	0.2	0.70745	±	0.00001	-0.87	±	0.02
	NS8	021-ROV-01	2011	30.0	±	0.2	9.5	±	0.2	0.70813	±	0.00001	-		
	NS11	047-ROV-03	2011	30.2	±	0.1	9.8	±	0.1	0.70792	±	0.00001	-0.90	±	0.02
	NS11	047-ROV-04	2011	28.1	±	0.1	8.5	±	0.1	-			-0.93	±	0.01

Table 1
(continued)

Edifice		Working ID	Year of sampling	$\delta^{11}B^b$	±	2SD	δ^7Li	±	2SD	$^{87}Sr/^{86}Sr^a$	±	2se	$\delta^{26}Mg$	±	2SD
				(‰)			(‰)						(‰)		
black smoker fluids															
North Su	NS3	J2-223-IGT7	2006	16.0	±	0.1	5.8	±	0.1	0.70471	±	0.00001	-		
	NS5	J2-227-IGT2	2006	17.7	±	0.1	6.0	±	0.2	0.70475	±	0.00001	-		
	NS5	J2-227-M2	2006	22.1	±	0.1	6.8	±	0.1	0.70582	±	0.00001	-		
	NS6	J2-227-IGT3	2006	17.0	±	0.1	5.7	±	0.2	0.70444	±	0.00001	-		
	NS6	J2-227-M4	2006	17.5	±	0.1	5.9	±	0.3	0.70460	±	0.00001	-		
	NS7	019-ROV-01	2011	18.3	±	0.1	5.9	±	0.3	0.70487	±	0.00001	-		
	NS10	045-ROV-02	2011	18.7	±	0.1	6.1	±	0.1	0.70516	±	0.00001	-		
bottom SW		J2-228-M4	2006	39.6	±	0.0	31	±	0.13	0.70916	±	0.00001	-0.87	±	0.03

mm, mmol/kg; µm, µmol/kg; "—" not determined; SW, seawater.
[a]Previously reported by: Tivey et al. (2006), Craddock et al. (2010), Reeves et al. (2011) and Seewald et al. (2015) for fluids collected in 2006. [b]Previously reported by Wilckens et al. (2018).

0.000044 [$2SD_{mean}$, n = 1,596]; GeoRem database; query October 2019; http://georem.mpch-mainz.gwdg.de). To verify the chemical separation and digestion technique used in this study, the basalt reference material BHVO-2 was also separated and analyzed. The results for BHVO-2 ($^{87}Sr/^{86}Sr$ = 0.70347 ± 0.00002 [$2SD_{mean}$, n = 2]) are within analytical uncertainty of literature values ($^{87}Sr/^{86}Sr$ = 0.70348 ± 0.00006 [$2SD_{mean}$, n = 80]; GeoRem database, query July 2017; http://georem.mpch-mainz.gwdg.de).

For Li isotope analysis at least 100-ng Li was loaded onto the column. Li was separated from its sample matrix using a two-step column separation detailed in Hansen et al. (2017) and modified after Moriguti and Nakamura (1998). Separated Li fractions were regularly checked for their purity and measured on a ThermoFisher Scientific Neptune Plus multicollector ICP-MS (MC-ICP-MS) equipped with a stable introduction system and a high-efficiency x-cone. Li isotope ratios were measured using the standard-sample bracketing method in 25-ng/g Li solutions with the reference material L-SVEC (NIST RM 8545; Flesh et al., 1973) as the bracketing standard. Li isotope ratios are reported in delta δ^7Li (‰) notation relative to L-SVEC. Procedural blanks were lower than 0.01% and hence do not affect the sample composition. The instrumental precision and internal long-term repeatability for δ^7Li was ±0.1‰ ($2SD_{mean}$, n = 17), obtained by the repeated analysis of L-SVEC. The δ^7Li value of an internal laboratory seawater standard (bottom seawater from SuSu Knolls) (δ^7Li of 31.1‰ ± 0.2‰ [$2SD_{mean}$, n = 5]) is in agreement with literature values for IAPSO seawater (e.g., +30.9‰ ± 0.1‰ [$2SD_{mean}$, n = 46], Huang et al., 2010; +31.2‰ ± 0.9‰ [$2SD_{mean}$, n = 44], Pogge von Strandmann et al., 2010). The basalt reference material BHVO-2 produced a δ^7Li value of 4.3‰ ± 0.3‰ ($2SD$, n = 2), which is within the range of published isotope values (4.3‰ ± 0.5‰ [$2SD_{mean}$, n = 7], Gao & Casey, 2011; 4.4‰ ± 0.8‰ [$2SD_{mean}$, n = 11], Genske et al., 2014). The uncertainty of the samples is reported as two standard deviation ($2SD$), based on preparation of replicates and on multiple analyses.

Approximately 1.5-µg Mg was separated from the sample matrix using a two-step column separation based on published distribution coefficients for the resin AG 50W X8, 200–400 mesh (after Strelow, 1960; Strelow et al., 1965). The first separation step was performed with 1 ml of the Bio-Rad cation exchange resin AG 50W X8 (200–400 mesh) in Bio-Rad Bio-Spin® columns in 1 M HCl. For the second separation step, the same columns and resin volumes were used, but the separation was done in 1 M HNO_3. The reliability of each chemical session was routinely checked with procedural blanks and reference materials. Procedural blanks were lower than 80 pg and thus did not affect isotope ratios of the samples (<0.1% of sample). To monitor loss of Mg during sample preparation, the head and tail of each Mg fraction was checked for its Mg concentration and the Mg fractions were checked for their purity.

Mg isotope measurements were performed on a ThermoFisher Scientific Neptune Plus MC-ICP-MS equipped with a stable introduction system and a high-efficiency x-cone. Pure Mg solutions were adjusted

to Mg concentrations of 200 ng/g. Samples were measured using the standard-sample bracketing method with a pure Mg ICP standard (Alfa Aesar Magnesium plasma standard solution, Specpure) as the bracketing standard. Each sample was analyzed at least three times. To evaluate single measurement sequences and to convert Mg isotope ratios into the DSM-3 scale, the international reference materials DSM-3 and Cambridge-1 (Cam-I) were analyzed in every sequence. The conversion of Mg isotope ratios into the DSM-3 scale was done using the following expression by Young and Galy (2004): $(\delta^{26}Mg_{DSM\text{-}3})_{sample} = (\delta^{26}Mg_{MgICP})_{sample} + (\delta^{26}Mg_{DSM\text{-}3})_{MgICP} + 0.001(\delta^{26}Mg_{MgICP})_{sample}\,(\delta^{26}Mg_{DSM\text{-}3})_{MgICP}$.

The instrumental precision and internal long-term repeatability for δ^{26}Mg was ±0.09‰ ($2SD_{mean}$, $n = 8$), obtained by the repeated analysis of the reference material Cambridge-I (Cam-I). δ^{26}Mg values for an internal seawater standard (bottom water SuSu Knolls) ($\delta^{26}Mg = -0.87‰ \pm 0.02‰$ [$2SD$, $n = 3$]) and Cam-I ($\delta^{26}Mg = -2.56‰ \pm 0.09‰$ [$2SD_{mean}$, $n = 8$]) are within analytical uncertainty in agreement with literature values, calculated from published values by Foster et al. (2010) (-0.82 ± 0.06 [$2SD_{mean}$, $n = 26$]) and Pogge von Strandmann et al. (2011) (-2.62 ± 0.04 [$2SD_{mean}$, $n = 43$]). The uncertainty of the samples is reported as two standard deviation ($2SD$), based on the preparation of duplicates and multiple analyses.

4. Results

4.1. Hydrothermal Fluids

Strontium, lithium, and magnesium concentration and isotope data from hydrothermal vent fluids collected from North Su and DESMOS are summarized in Table 1 together with previously published concentrations for SiO_2, Cl, SO_4, and B, and the isotope composition of B (Craddock et al., 2010; Reeves et al., 2011; Seewald et al., 2015; Seewald et al., 2019; Wilckens et al., 2018).

4.1.1. Hybrid Smoker Fluids

The two vent fluids sampled at DESMOS in 2006 can be termed as acid-sulfate fluids (Seewald et al., 2015). However, a strict classification of some of the collected vent fluids from North Su as either acid-sulfate (low pH, elevated SO_4, typically milky white smoke visible) or black smoker fluids (enriched in alkali elements, depleted in Mg and SO_4) is not possible. While the chemical composition of acid-sulfate fluids implies dilution of seawater with a magmatic fluid, the black smoker fluids indicate extensive chemical exchange with fresh rocks. North Su vents NS4 sampled in 2006 and NS8 and NS11 sampled in 2011 share characteristics of both acid-sulfate and black smoker fluids (Seewald et al., 2019). Relative to the acid-sulfate fluids (Mg = 39.2–45.4 mmol/kg), NS8 and NS11 samples have similarly high Mg contents (40.8–44.2 mmol/kg), while those at NS4 are substantially lower (23.5–24.2 mmol/kg), yet none approach near zero Mg concentrations. All three are also characterized by low pH (≤2.5). SO_4 concentrations are either similar to seawater or slightly elevated and do not extrapolate to zero Mg as in the case of nearby summit black smoker fluids, which are trend toward a near-zero SO_4 and Mg composition (Seewald et al., 2019). Zero-Mg extrapolated end-member Cl contents (579, 641, and 618 mmol/kg, respectively) and Na contents (484, 536, and 451 mmol/kg, respectively) of NS4, NS8, and NS11 samples are all elevated compared to those of seawater and more similar to the range of summit smoker Cl and Na end-members (550–785 and 446–605 mmol/kg, respectively). In contrast, extrapolated (zero-Mg) Cl and Na contents for the acid-sulfate fluid samples are extremely low with values <152 and <53 mmol/kg, respectively. The alkali elements are clearly enriched in all NS4, NS8, and NS11 fluid samples (e.g., Seewald et al., 2015). These hybrid chemical characteristics imply that these fluids likely formed as some novel variant of a three-component mixture of magmatic fluid, seawater, and a convective seawater-derived hydrothermal fluid typical of the black smoker fluids. Hence, in this study we follow Seewald et al. (2019) in referring to this third class of compositions as "hybrid" smokers to distinguish these fluids from strictly acid-sulfate (i.e., purely magmatic) fluids and more typical seawater-derived black smoker fluids venting at the North Su summit.

4.1.2. Physical and Chemical Properties of the 2011 North Su Vent Fluids

Physical and chemical properties of the DESMOS fluids and North Su fluids sampled in 2006 are published by Seewald et al. (2015, 2019). In 2011, five additional vent sites were sampled at North Su volcano (BAMBUS cruise, SO-216). Similar to the 2006 fluids, fluids venting at North Su can be categorized as acid-sulfate (NS9), hybrid smoker (NS8 and NS11), and black smoker (NS7 and NS10) fluids. The most vigorously venting site sampled in 2006 (comprising vents NS1 and NS2) was buried prior to the 2011 cruise by products of a volcanic cryptodome eruption (Thal et al., 2016). In 2011, a previously unexplored vent area,

named Sulfur Candles, was also sampled. This area is characterized by meter-thick flows of molten sulfur, with white smoke and liquid CO_2 bubble venting (Bach et al., 2011; Reeves et al., 2015; Thal et al., 2016).

The temperatures (312 to 332 °C), pH (3.2 to 4.8), and chemical compositions of black smoker fluids from 2011 are consistent with those of the fluids from 2006 (Seewald et al., 2019). Mg and SO_4 concentrations decrease linearly to near zero, whereas Cl, alkali, and alkaline elements become enriched with decreasing Mg concentrations. Hybrid smoker fluids from 2011 have lower temperatures (129 to169 °C), lower pH (1.9 to 2.4), and higher Mg concentrations compared to those of the black smoker fluids and to those of the NS4 hybrid fluid from 2006. Cl and SO_4 concentrations are similar to NS4 fluid with near seawater abundances. The most striking difference of the acid-sulfate fluids collected in 2011 is the associated venting of liquid CO_2 bubbles that were not observed at the NS1 or NS2 vents in 2006 (Reeves et al., 2015). Maximum temperatures (103 °C), pH, and the chemical compositions in 2011 do, however, broadly resemble those of the acid-sulfate fluids collected in 2006 (Table 1).

4.1.3. Strontium Concentration and Isotope Ratios

The acid-sulfate fluids are characterized by Sr concentrations of 59 to 87 μmol/kg, slightly lower than the seawater concentration of 91 μmol/kg. The hybrid smoker fluids are both enriched and depleted in Sr relative to seawater (73 to100 μmol/kg). In contrast, all black smoker fluids are enriched in Sr with concentrations of 151 to 410 μmol/kg. $^{87}Sr/^{86}Sr$ values in all fluids are lower than that in seawater (0.70916), ranging from 0.70870 to 0.70902 for the acid-sulfate fluids, 0.70739 to 0.70813 for the hybrid smoker fluids, and 0.70444 to 0.70582 for the black smoker fluids.

4.1.4. Lithium Concentration and Isotope Ratios

Measured Li concentrations in the acid-sulfate fluids from DESMOS (21 to 31 μmol/kg) and North Su (27 to 41 μmol/kg) are close to or exceed the concentration in seawater (28 μmol/kg). In contrast, Li concentrations in the hybrid and black smoker fluids exceed the seawater abundance with concentrations of 122 to 419 and 348 to 806 μmol/kg, respectively. δ^7Li values in the acid-sulfate fluids from DESMOS are close to that of seawater (+31.0‰) with values between +29.2‰ and +30.1‰, whereas those from North Su have slightly lower δ^7Li values between +17.2‰ and +24.3‰. The hybrid and black smoker fluids have even lower δ^7Li values of +6.2‰ to +9.8‰ and of +5.7‰ to +6.8‰, respectively.

4.1.5. Mg Concentration and Isotope Ratios

Mg concentrations in the hybrid smoker and acid-sulfate fluids from North Su are all depleted relative to seawater (52.4 mmol/kg). Fluid samples from the NS4 vent have the lowest Mg concentrations (23.5 to 24.2 mmol/kg), whereas the NS1 samples have the highest Mg concentrations (49.6 to 50.4 mmol/kg). Mg concentrations in the samples from DESMOS are similarly high, ranging from 44.9 to 50.0 mmol/kg. Mg isotope ratios were analyzed in the hybrid smoker and acid-sulfate fluids with elevated Mg concentrations, to confirm whether Mg is seawater or basement derived. $\delta^{26}Mg$ values in the hybrid smoker and acid-sulfate fluids define a small range from −0.82‰ to −0.93‰. Bottom seawater, which was collected close to the sample sites in the EMVZ, has a $\delta^{26}Mg$ value of −0.87‰.

4.2. Volcanic Rock Samples

Lithium and strontium concentration and isotope data from eight volcanic rocks from different sites at DESMOS and SuSu Knolls (North Su and South Su) together with previously published concentrations for SiO_2 (Beier et al., 2015; Wilckens et al., 2018) are summarized in Table 2.

We separated the rocks into three groups according to the extent and style of alteration: (1) fresh volcanic rocks without alteration; (2) volcanic rocks characterized by (advanced) argillic alteration with mineral assemblages of quartz, pyrophyllite, and natroalunite; and (3) volcanic rocks characterized by argillic and sericitic alteration with variable proportions of pyrite, natroalunite, pyrophyllite, mica, talc, cristobalite, and quartz.

Li concentrations and δ^7Li values range from 2.7 to 10.1 μg/g and +4.9‰ to +5.1‰ in the rocks of group 1, respectively. The altered volcanic rock samples (groups 2 and 3) have lower Li concentrations between 0.2 and 1.4 μg/g with δ7Li values of +3.0‰ (group 3) and between +4.9‰ and +17.8‰ (group 2). Strontium concentrations in the fresh volcanic rocks range from 422 to 442 μg/g with $^{87}Sr/^{86}Sr$ between 0.70366 and 0.70420. The altered samples of groups 2 and 3 have a more variable Sr contents, ranging between 226 and 616 μg/g, and show $^{87}Sr/^{86}Sr$ values between 0.70470 and 0.70673.

Table 2
B, Li, and Sr Concentrations and Isotope Ratios of Fresh and Altered Rocks From the Manus Basin

Sample	Alteration degree/group	SiO_2[a] (wt%)	Li[a] (μg/g)	Sr[a] (μg/g)	B[b] (μg/g)	δ^7Li	± (‰)	2*SD*	$^{87}Sr/^{86}Sr$	±	2*SD*	$\delta^{11}B$[b]	± (‰)	2*SD*
J2-221-16-R2	Fresh/1	60	2.7	423	11.8	5.5	±	0.4	0.70367	±	0.00001	8.3	±	0.1
J2-224-10-R1	Fresh/1	63	10.1	442	23.7	4.4	±	0.3	0.70366	±	0.00001	8.0	±	0.1
J2-220-13 R1	Slightly altered/1	58	8.5	422	12.1	4.7	±	0.2	0.70420	±	0.00004	8.8	±	0.1
J2-221-4-R1	Altered/2	64	1.4	226	9.4	7.8	±	0.2	0.70470	±	0.00004	9.0	±	0.1
J2-224-2-R1	Altered/2	80	0.2	616	1.8	17.8	±	0.0	0.70673	±	0.00007	20.0	±	0.1
J2-220-8-R1	Altered/2	67	3.0	541	18.9	5.8	±	0.4	0.70514	±	0.00007	5.3	±	0.1
J2-220-9-R1	Altered/2	68	0.4	138	1.8	12.2	±	0.3	0.70547	±	0.00006	9.6	±	0.1
J2-221-6-R1	Altered/3	59	0.7	356	11.6	3.0	±	0.1	0.70501	±	0.00018	7.0	±	0.3

[a]Fresh volcanic rocks from the Manus Basin were previously reported by Beier et al. (2015). [b]data previously reported by Wilckens et al. (2018).

5. Discussion

5.1. Source of Mg in Acid-Sulfate Fluids

The chemical compositions of acid-sulfate fluids in the Manus Basin are primarily explainable by direct injection of a magmatic fluid into cold seawater residing in voids of the volcanic basement, with water-rock interaction involving highly altered basement (advanced argillic alteration) in the absence of convective hydrothermal seawater circulation (Seewald et al., 2015). Similar to those in seawater, K/Mg and Na/Mg ratios (Table S1 in the supporting information) in the acid-sulfate fluids from the EMVZ have been used to imply limited reaction with fresh volcanic substrate and a seawater origin for these elements (Seewald et al., 2015). Mg concentrations in acid-sulfate fluids from DESMOS and North Su are mainly close to seawater Mg and are up to 30 times higher than the Mg concentrations in black smoker fluids from the same study area (Table 1) (Reeves et al., 2011; Seewald et al., 2015). Due to the extreme acidity of acid-sulfate fluids, high Mg concentrations in the first acid-sulfate fluids discovered at DESMOS were initially thought to reflect dissolution of Mg-bearing silicates in the discharge zone (Gamo et al., 1997). Since Mg-bearing minerals are scarce or absent in the highly altered basement at DESMOS and North Su (Binns et al., 2007; Gena et al., 2001; Hrischeva et al., 2007; Lackschewitz et al., 2004; Paulick & Bach, 2006), and fluids there display near-seawater K/Mg and Na/Mg ratios, Seewald et al. (2015) inferred that Mg in acid-sulfate fluids is primarily seawater derived. The Mg-depletion of the altered basement relative to fresh precursor rocks implies that extensive leaching of Mg occurs during hydrothermal alteration. Thus, it is possible that Mg-leaching from the basement may influence the Mg isotope composition of at least some acid-sulfate fluids in scenarios where upflow zones are still relatively fresh or unaltered (e.g., due to incipient discharge or opening of new fluid pathways). It is equally plausible to assume that Mg-silicates have not been precipitated from the acid-sulfate-type fluids. Considering that Mg solubility in hydrothermal systems can be represented by the reaction $3Mg^{2+} + 4SiO_2(aq) + 4H_2O = Mg_3Si_4O_{10}(OH)_2 + 6H^+$, where talc ($Mg_3Si_4O_{10}(OH)_2$) is used as an analog for more compositionally complex Mg phases (Seyfried, 1987), precipitation of hydrous Mg-silicates should be inhibited by the low pH of acid-sulfide fluids.

Due to the large difference in the isotopic composition of Mg in seawater ($\delta^{26}Mg = -0.89‰ \pm 0.18‰$ [2*SD*, $n = 44$], Pogge von Strandmann et al., 2008) and oceanic basalts ($\delta^{26}Mg = -0.26‰ \pm 0.07‰$ [2*SD*, $n = 110$], Teng et al., 2010), the isotopic composition of Mg in acid-sulfate fluids is a powerful tool for investigating its origin. Altered oceanic crust of MORB composition has more variable $\delta^{26}Mg$ values dependent on the type and extent of alteration, but average $\delta^{26}Mg$ values range between −0.25‰ and 0.00‰ (Huang et al., 2015, 2018). Mg isotope ratios in island arc lavas may be slightly higher than those in MORB due to fluid-peridotite interactions in the mantle wedge and have $\delta^{26}Mg$ values between −0.25‰ and −0.10‰ (Teng et al., 2016). We can thus reasonably assume that all possible basement compositions are likely to have substantially higher $\delta^{26}Mg$ values than are seawater. Hence, Mg leached from the volcanic basement in the EMVZ can be expected to shift the isotopic composition of vent fluids toward higher $\delta^{26}Mg$ values. The Mg isotope ratios of the acid-sulfate and hybrid smoker fluids are indistinguishable from that of seawater

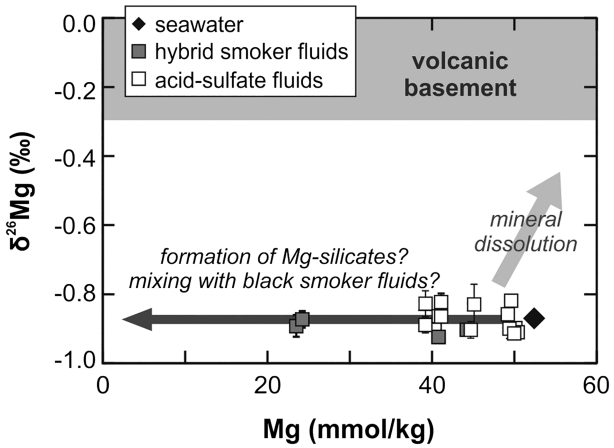

Figure 3. Mg concentration against Mg isotope composition of acid-sulfate- and hybrid smoker-type fluids. Gray area indicates the composition of the oceanic crust. Arrows indicate expected compositional changes due to mineral dissolution (light gray arrow), and formation of Mg-silicates during water-rock interaction or mixing with "zero-Mg" black smoker fluids (dark gray arrow). Despite their huge variation in their Mg concentrations, all acid-sulfate and hybrid smoker fluids have δ^{26}Mg values similar to that of seawater. This implies that the high Mg concentrations of acid-sulfate fluids cannot be explained by dissolution of basement minerals but reflect either incomplete Mg loss during water-rock interaction or mixing with "zero-Mg" fluids.

(Fig. 3) and therefore support the hypothesis by Seewald et al. (2015) that Mg is mainly seawater derived in the 2006 and 2011 hydrothermal fluids from North Su and DESMOS. However, due to analytical uncertainties associated with the Mg concentrations and isotope measurements, we cannot preclude that small amounts of Mg were leached from the basement.

The intermediate Mg concentrations in samples of the hybrid smoker fluid NS4 (23.5−24.2 mmol/kg, about half that of the other acid-sulfate fluids) imply partial loss of Mg from the circulating fluid. The Mg isotope ratios of these fluids are indistinguishable from that of seawater, which implies that either (i) the fluids either represent a subsurface mixture between a pure zero-Mg end-member black smoker fluid and unmodified Mg-replete seawater, consistent with other hydrothermal fluids in the Manus Basin (Reeves et al., 2011; Seewald et al., 2019), or (ii) Mg removal from seawater during hydrothermal circulation was incomplete but occurred without substantial isotopic fractionation during Mg incorporation into the volcanic basement. Minimal Mg isotope fractionation during hydrothermal Mg uptake by rocks would be consistent with evidence for only very modest overall increases in Mg isotope ratios (+0.25‰) of altered oceanic crust basalt relative to fresh MORB, as documented by Huang et al. (2015). Removal of Mg from seawater during hydrothermal circulation (i.e., by forming Mg-hydroxysilicates) through back-arc crust may also proceed with a similarly negligible isotope effect, leaving the residual fluid δ^{26}Mg relatively unchanged. As a consequence, the near-seawater δ^{26}Mg values of all acid-sulfate- and hybrid smoker-type fluids presented here cannot necessarily differentiate (e.g., in the case of NS4) such nonfractionating partial Mg uptake from subsurface admixing of Mg-replete seawater with a zero-Mg acid-sulfate or hybrid smoker fluid end-member, at least at DESMOS and North Su. In other back-arc magmatic-hydrothermal systems, δ^{26}Mg may, however, still trace Mg leaching from basement rocks even if Mg concentrations are lower than seawater.

5.2. Evidence From Sr Isotope Ratios for Subseafloor Fluid-Rock Interaction

Sr isotope ratios (^{87}Sr/^{86}Sr) are a powerful tool for understanding water-rock interaction in hydrothermal systems (e.g., Albarède et al., 1981; Berndt et al., 1988). Similar to Mg isotope ratios, Sr isotope ratios in seawater and the oceanic crust are distinct (e.g., Davis et al., 2003), and Sr in vent fluids is mainly modified through high-temperature water-rock interaction. Leaching of Sr from the volcanic basement is most intense at temperatures above 250 °C (James et al., 2003), resulting in a rock-derived isotopic signal in the fluids. In addition, Sr in vent fluids can also be influenced by precipitation or dissolution of anhydrite minerals during hydrothermal circulation or admixing with seawater. Precipitation of anhydrite only affects the Sr concentration of the hydrothermal, fluid while the isotopic composition of the fluids remains unchanged (Berndt

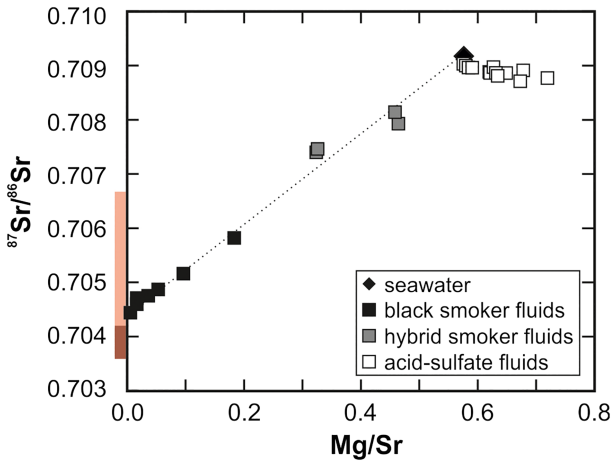

Figure 4. Plot of Mg/Sr versus $^{87}Sr/^{86}Sr$ in the different fluids from the EMVZ. The brown areas close to the *y*-axis indicate the isotope composition of fresh (dark brown) and altered (light brown) rocks. The figure shows that the black smoker fluids define a trend toward a rock-derived signal. Hybrid smoker fluids have a similar end-member (indicated by the dotted line) but may reflect admixing with a seawater-like fluid or lower *w*/*r* ratios and low reaction temperatures. The high Mg/Sr ratios and seawater-like $^{87}Sr/^{86}Sr$ of the acid-sulfate fluids, however, imply limited contribution of Sr leached from the basement (basement alteration and high *w*/*r* ratios) and absence of Sr in the magmatic fluid end-member (see text for further details).

et al., 1988, Voigt et al., 2018). In contrast, the dissolution of anhydrite and admixing with seawater can directly influence the concentration of Sr and its isotopic composition. Both precipitation and dissolution, can, however, make the classical application of $^{87}Sr/^{86}Sr$ versus Mg/Sr systematics problematic for calculating *w*/*r* ratios for some mixed fluids (Reeves et al., 2011).

Figure 4 shows that the black smoker fluids at North Su have a uniform end-member $^{87}Sr/^{86}Sr$ of about 0.7045. This indicates water-rock interaction at high temperatures with fresh volcanic basement, which has $^{87}Sr/^{86}Sr$ ratios of about 0.7037 (Beier et al., 2015). The hybrid smoker fluids at North Su (NS4; NS8 and NS11) have more radiogenic $^{87}Sr/^{86}Sr$ (0.70739 to 0.70813) and Sr concentrations similar to or lower than that of seawater. Although these fluids plot near to the $^{87}Sr/^{86}Sr$ mixing line of the North Su end-member and seawater, they deviate from the line beyond typical analytical uncertainty (~0.00001) and yield a broad range of apparent end-member values at Mg/Sr = 0 (0.7038 to 0.7054). The acid-sulfate fluids from North Su and DESMOS have even more radiogenic $^{87}Sr/^{86}Sr$ with an average ratio of 0.7089 and Sr concentrations slightly lower than that in seawater. Since acid-sulfate and hybrid fluids invariably comprise a three-component mix of magmatic fluid (likely depleted in Sr), seawater-derived hydrothermal fluid, and admixed seawater, in unclear proportions and with the possibility for anhydrite dissolution effects (Seewald et al., 2015), extrapolation to a Mg/Sr of zero may not be reasonable. Many of the measured acid-sulfate fluids are depleted in Sr relative to mixing between a Sr-free magmatic fluid and seawater, presumably reflecting Sr loss to anhydrite.

In general, $^{87}Sr/^{86}Sr$ in hydrothermal fluids can be used to constrain *w*/*r* ratios during water-rock interaction (e.g., Berndt et al., 1988). Calculation of *w*/*r* ratios in the black, hybrid, and acid-sulfate fluids from the Manus Basin may be a poor reflection of realistic water fluxes, however, since Sr can be influenced by several processes. In general, near-seawater $^{87}Sr/^{86}Sr$ ratios and low Sr contents in acid-sulfate fluids may reflect three distinct possibilities: (1) limited contribution of Sr leached from basement, perhaps due to high *w*/*r* ratios or low reaction temperatures; (2) Sr-bearing phases in the basement are completely altered, leaving low Sr concentrations and/or Sr isotopic compositions similar to that of seawater; or (3) the Sr concentration in the magmatic fluid end-member is extremely low, and Sr in venting acid-sulfate fluids is therefore dominated by the isotopic composition of seawater.

It is likely that the Sr isotopic compositions of the acid-sulfate fluids and to some extent also the hybrid fluids from North Su and DESMOS are affected by a combination of these possibilities. (1) and (3) seem more likely, however, given that even at high temperatures, the extent of alteration of Sr-bearing mineral

phases appears to be relatively minor, at least under conditions encountered by typical black smoker fluids (Berndt et al. 1988). Nevertheless, the altered volcanic rock samples from the Manus Basin show a pronounced shift toward higher Sr concentrations and higher $^{87}Sr/^{86}Sr$ compared to the fresh "group 1" volcanic rocks, which implies that water-rock interaction has an effect on Sr in the basement. This shift can, however, be explained by the formation of anhydrite and thus Sr loss from the acid-sulfate fluids. The broad similarity in the $^{87}Sr/^{86}Sr$ end-members identified for the black and hybrid smoker fluids (Fig. 4) points to a more pronounced entrainment of seawater for the hybrid fluids and some contribution of Sr leached during water-basement interaction. To further identify the processes and conditions that formed those fluids, additional proxies for water-rock interaction or basement alteration are necessary.

5.3. Li isotopes as a Proxy for Basement Alteration

Li is a fluid-mobile element, and while it is taken up from seawater into basalt at low to moderate temperatures, it is leached from oceanic crust during high-temperature water-rock interaction (Chan et al., 1992; Chan et al., 2002; James et al., 2003; Seyfried et al., 1984; Verney-Carron et al., 2015). Li concentrations and δ^7Li values in hydrothermal vent fluids are mainly influenced by (1) Li concentrations and isotope ratios of the basement (fresh versus altered basement) (Chan et al., 1992; Chan et al., 2002), (2) w/r ratios during water-rock interaction (Araoka et al., 2016), and/or (3) the reaction temperature (James et al., 2003; Millot et al., 2010; Seyfried et al., 1984). Equilibrium Li isotope fractionation factors between solid and fluid range from $\alpha_{rock\text{-}fluid} = 0.992$ at 200 °C to 0.995 at 300 °C and 0.997 at 400 °C (Millot et al., 2010). Li may therefore be a sensitive tracer of water-rock interaction and basement alteration in acid-sulfate fluids.

Low δ^7Li values (5.8‰–9.8‰) and elevated Li concentrations (122–833 μmol/kg) of the hybrid and black smoker fluids from North Su relative to seawater are in agreement with other black smoker fluids from the Western Pacific (Araoka et al., 2016) and reflect high-T (>250 °C) water-rock interaction at low w/r ratios. Although the acid-sulfate fluids from DESMOS are also characterized by δ^7Li values that are below those of seawater, the Li concentrations are similar or below seawater values, which can be indicative for water-rock interaction at lower temperatures around 150 °C (James et al., 2003). Furthermore, the low Li concentrations are also broadly in agreement with mixing between seawater and a virtually alkali-free magmatic fluid end-member (Seewald et al., 2015), consistent with low Sr contents in the same fluids. These minor changes in concentration aside from lower δ^7Li values in all acid-sulfate fluids, however, suggest that some Li-exchange during water-rock reaction occurs in the acid-sulfate fluids at DESMOS. Lithium exchange between basement and acid-sulfate fluids is supported by the trend toward low Li concentration and high δ^7Li values in the argillic-altered volcanic rocks (group 2) from the Manus Basin (Figure 6b).

The acid-sulfate fluids at North Su, on the other hand, display Li concentrations similar to or enriched relative to seawater (NS1, NS2, and NS9; Table 1). They also have elevated concentrations of other fluid-mobile elements, for example, Rb and Cs (Seewald et al., 2015). Interestingly, Li isotope ratios in the acid-sulfate fluids from North Su are variable and are clearly distinct from those of seawater. These differences in the Li systematics are contrasted by similar Sr isotope ratios in both acid-sulfate vent sites (Figure 5a). Similar venting temperatures in the measured acid-sulfate fluids from NS1 and NS9 within North Su (49–103 °C) and from DESMOS (70–117 °C) do not support temperature-related differences in water-rock reaction as a factor in the diverging Li abundances and isotope fractionation between fluid and basement in the two sites. Instead, water-rock interaction with a less altered (fresher) basement (and thus higher Li concentrations) at North Su best explains the observed offsets. This hypothesis is supported by evidence for ongoing volcanic activity at North Su (Thal et al., 2016), which indicates the near-seafloor emplacement of very recent (i.e., post-2006) fresh rock. In contrast, there was no conspicuous evidence for recent volcanic activity in the caldera wall site of DESMOS, where activity has persisted in a relatively localized area at the Onsen site from 1995 to 2006, albeit with an apparent gradual increase in SO_2 emitted in acid-sulfate fluids there (Gamo et al., 1997; Seewald et al., 2015). Nevertheless, since there is a broad range of temperatures (48 to 215 °C) in the acid-sulfate fluids from North Su, we cannot exclude temperature-related differences in δ^7Li in the acid-sulfate fluids from North Su, but there is no correlation between venting temperatures and Li systematics in the fluids. The absence of a uniform trend between venting temperature and δ^7Li implies that the different Li isotope compositions in the acid-sulfate fluids cannot solely originate from differences in the reaction temperature. This supports the idea that Li instead reflects the alteration state of the oceanic crust

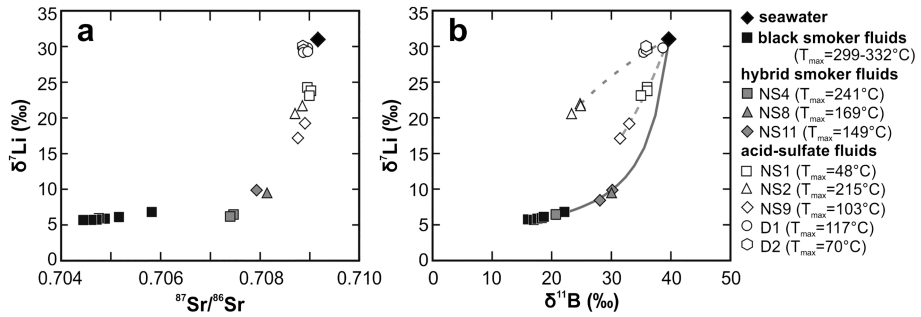

Figure 5. (a) $^{87}Sr/^{86}Sr$ and δ^7Li values in acid-sulfate, hybrid, and black smoker fluids compared to those of seawater. Black smoker fluids reflect water-rock interaction (low *w*/*r*) with fresh or slightly altered basement. Acid-sulfate fluids from DESMOS (D1 and D2) plot close to seawater, implying almost no water-rock interaction or water-rock interaction with altered rock, whereas the significant decrease in δ^7Li in the acid-sulfate and the coupled decrease in δ^7Li and $^{87}Sr/^{86}Sr$ in the hybrid smoker fluids from North Su indicate increasing water-rock interaction with lower *w*/*r* ratios and/or less altered basement. (b) $\delta^{11}B$ and δ^7Li in the hybrid and black smoker fluids define the same curve and imply water-rock interaction at low *w*/*r* ratios with fresh rock. The different mixing lines for the acid-sulfate fluids, however, may reflect changes in water-to-rock ratios and/or a heterogeneously altered basement (see text for further details).

and/or *w*/*r* ratios, as well as any contributions of Li from seawater admixed in the subsurface during fluid ascent.

5.4. Modeling of Water-Rock Interaction

To assess if Li isotope ratios in acid-sulfate fluids trace the alteration degree of the basement, we apply the mass balance model of Araoka et al. (2016) that is based on the models of Verney-Carron et al. (2015) and Magenheim et al. (1995). To calculate the Li concentrations [Li] and isotope ratios ($^7Li/^6Li$) of the acid-sulfate fluids (f) and altered rocks (a), we assume leaching of Li from the primary mineral phases and partitioning of Li into the fluid and alteration phases considering isotopic fractionation (α) at steady state in a closed system, using the Li concentrations and isotope ratios of the initial rock (i), the starting fluid (s), the water/rock mass ratio (*w*/*r*) and the Li distribution coefficient (D_{Li}) between liquid and solid phases during water-rock interaction.

$$[Li]_f = \frac{([Li]_r + w/r[Li]_s)}{(K + w/r)} D_{Li} = \frac{[Li]_a}{[Li]_f}\left(\frac{^7Li}{^6Li}\right)_f = \frac{\left(\left(\frac{^7Li}{^6Li}\right)_r [Li]_r + w/r\left(\frac{^7Li}{^6Li}\right)_s [Li]_s\right)}{([Li]_r + w/r[Li]_s)} \frac{([Li]_a + w/r[Li]_f)}{(\alpha[Li]_a + w/r[Li]_f)}$$

The volcanic rock sample J2-224-10 R1 was selected as initial rock composition $[Li]_r$ and $(^7Li/^6Li)_r$. This rock sample is a fresh, vesicular lava with andesitic composition and was chosen because it shows no visible signs of alteration. The parameters used to generate the different modeled curves in Figure 6 are summarized in Table 3.

Using the experimentally determined Li distribution coefficients and isotope fractionation factors 0.35 and 0.994 for 260 °C, 0.32 and 0.995 for 300 °C, 0.27 and 0.996 for 350 °C, and 0.23 and 0.997 for 400 °C (Millot et al., 2010), the compositions of the black smoker and hybrid smoker fluids are in agreement with all modeled corves (Figure 6a). The modeled composition of the altered rock agrees as well with the measured value for the altered rock of group 3 that has mineral assemblages implying high-temperature water-rock interaction (Figure 6b). However, both the acid-sulfate fluids (Figure 6a) and the group 2 volcanic rocks (Figure 6b) do not match the modeled curves. Instead, we propose a two-stage model that can explain both the composition of the acid-sulfate fluids (Figure 6c) and group 2 altered volcanic rocks (Figure 6d). In a first step, unmodified seawater mixes with Li-free magmatic fluids, which leads to lower Li concentrations but unchanged δ^7Li values. In a second step, the fluid reacts with the basement. Due to the relatively low temperatures and depletion of Li in altered basement, the fluids leach less Li from the basement compared to the black smoker fluids. The model further implies that there is no or negligible Li isotope fractionation during leaching of Li and/or Li incorporation into secondary phases at acid-sulfate conditions. This is in contrast to observations that Li incorporation during formation of secondary minerals at low and

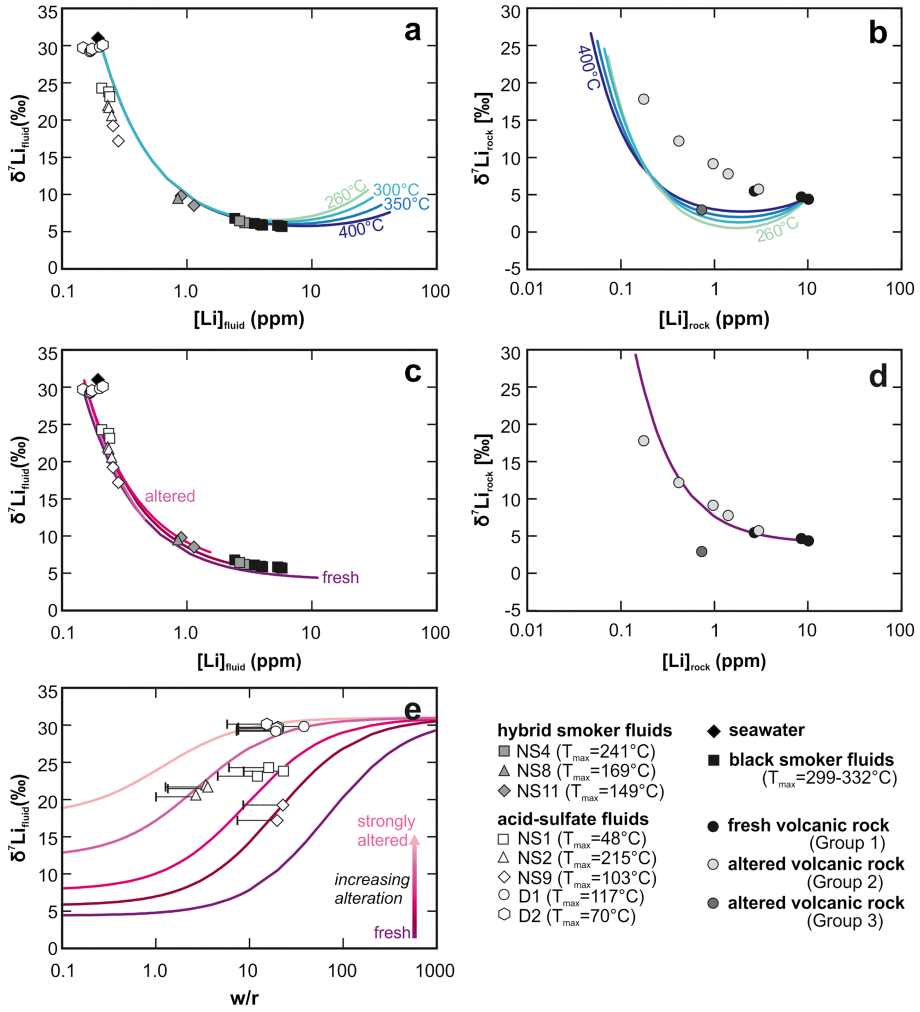

Figure 6. Modeled (lines) and measured (symbols) Li concentrations and isotope ratios in the (a, c) fluids and (b, d) rocks. (a) and (b) show that the black smoker fluids and the altered volcanic rock of group 3 fit the model using Li isotope fractionation factors and Li distribution coefficients for high-temperature (>350 °C) water-rock interaction. (c) and (d) show that the acid-sulfate fluids and (advanced) argillic altered rocks (group 2) can be explained by a two-step model that assumes mixing of seawater with a zero-Li magmatic fluid and subsequent water-rock interaction without Li isotope fractionation and with higher solid/fluid Li distribution coefficients. (e) The relationship between *w/r* and δ^7Li values in the fluids. The curves were calculated using the same parameter as in (c) and (d), and the different curves reflect different basement compositions ranging from fresh to strongly altered basement. *w/r* ratios for the fluids were calculated from B concentrations of fluids and fresh volcanic rocks. The error bars show the range of *w/r* ratios using lower B concentrations of the altered volcanic rocks. The combination of the modeled curves with fluid data shows that it is possible to distinguish between changing *w/r* ratios and the alteration degree of the basement for the different vent sites with a combination of B concentrations and Li isotope ratios (see text and Table 3 for further details).

high temperatures leads usually to an isotope fractionation of Li between fluid and solid phases (e.g., Araoka et al., 2016; Seyfried et al., 1984). Negligible Li isotope fractionation during dissolution of primary minerals is also observed during low-temperature processes, for example, weathering of silicate rocks (Pistiner & Henderson, 2003). The apparent lack of a Li isotope fractionation between the fresh and altered volcanic rocks in the Manus Basin might thus be related to a high net dissolution rate caused by the high acidity of the fluids and an absence of Li incorporation into alteration phases. Both is supported by the decrease in Li in the volcanic rocks from the Manus Basin with increasing degree of alteration (Table 2). Additionally, most of the identified alteration phases (e.g., cristobalite, native sulfur, and pyrite) in the altered volcanic rocks do not incorporate Li.

Table 3
Parameters Used to Model Fluids and Rock Compositions

Model	D_{Li}	α	$[Li]_s$ (μg/g)	δ^7Li_s (‰)	$[Li]_r$ (μg/g)	δ^7Li_r (‰)
High-temperature water-rock interaction						
260 °C	0.35[a]	0.994[a]	0.20	31.0	10	4.4
300 °C	0.32[a]	0.995[a]	0.20	31.0	10	4.4
350 °C	0.27[a]	0.996[a]	0.20	31.0	10	4.4
400 °C	0.23[a]	0.997[a]	0.20	31.0	10	4.4
Acid-sulfate water-rock interaction						
Fresh rock (J2-224-10-R1)	0.9	1	0.15	31.0	10	4.4
J2-220-8-R1	0.9	1	0.15	31.0	3	5.8
J2-221-4-R1	0.9	1	0.15	31.0	1	7.8
J2-220-9-R1 crust	0.9	1	0.15	31.0	0	12.2
J2-224-2-R1	0.9	1	0.15	31.0	0	17.8

[a]Previously reported by Millot et al. (2010).

Using the two-stage model and fresh volcanic rocks as basement composition, the Li composition in the fluids imply w/r ratios higher than 60, which would be indicative of limited water-rock interaction. However, using the composition of altered volcanic rocks, calculated w/r ratios decrease to ratios as low as 1. To further test whether the different Li compositions of the acid-sulfate fluids indicate different w/r ratios during water-rock interaction or a heterogeneously altered basement, we use an additional tracer for water-rock interactions.

5.5. Tracing Alteration With a Combination of Li and B Isotope Ratios

Boron in hydrothermal fluids is mainly controlled by B concentrations and isotope ratios of the basement rocks but may be influenced by addition of magmatic fluids, phase separation, and, similar to Li, by the alteration state of the oceanic crust. Although B in volcanic rocks can become depleted during advanced argillic alteration, B isotope ratios in most of the acid-sulfate fluids match those of the black and hybrid smoker fluids, indicating a subordinate control of basement alteration on B systematics of the fluids (Wilckens et al., 2018). Figure 5c shows the relationship between B and Li isotope ratios in different fluids from the EMVZ and the calculated mixing curves. In agreement with Sr and Li isotope ratios, the hybrid smoker fluids plot on a similar mixing trend as the black smoker fluids, providing additional confirmation that they are influenced by rock-dominated water-rock interaction with fresh oceanic crust. Fluids from DESMOS, from NS2, and those from NS1 and NS9 define distinct mixing trends (Figure 5b). Wilckens et al. (2018) suggested that the magmatic end-member of acid-sulfate fluids from NS9 are influenced by magmatic fluids and have considerably less B than have other fluids, which had more B added from water-rock interaction. However, there is no influence of magmatic fluids on the relationship between Li and B isotope ratios, implying that these effects might be too small to be seen in the heavily diluted seawater-magmatic fluid mixtures. As boron is less influenced by the alteration of the basement at acid-sulfate conditions in comparison with Li and magmatic inputs that appear to be relatively minimal (Wilckens et al., 2018), we use the B concentrations in the acid-sulfate fluids and fresh oceanic crust to calculate w/r ratios using a simple mass balance equation (Yamaoka et al., 2015):

$$w/r = \frac{[B]_f D_B - [B]_r}{[B]_s - [B]_f}$$

with the B concentration [B] of the acid-sulfate fluid (f), the initial rock composition (r), and the starting fluid (s) and the B distribution coefficient between liquid and solid ($D_B = 0.1$; Yamaoka et al., 2012). Since B in the volcanic rocks can get depleted during alteration (Table 2), the w/r ratios obtained from B concentrations are maximum w/r ratios of the fluids, and the possible range of w/r ratios considering lower B concentrations in the altered volcanic rock is given by error bars in Figure 6e.

Calculated w/r ratios obtained from B concentrations vary between 3 and 38, which is considerably lower than the w/r ratios obtained from Li concentrations using fresh volcanic rocks as basement

composition. The lower w/r ratios for the NS2 fluids compared to those of the other acid-sulfate fluids might be related to the higher reaction temperatures during water-rock interaction. The comparison of w/r ratios obtained from B with modeled δ^7Li values for reaction with fresh and altered volcanic rocks (Figure 6e) shows that the combination of B with Li isotope ratios in acid-sulfate fluids appear to be a promising tracer to assess the alteration of basement rock in back-arc hydrothermal systems. However, there are uncertainties in using the B distribution coefficient between solid and fluid phases of 0.1, which was determined for high-temperature water-rock interaction (Yamaoka et al., 2012). In addition, the influence of the basement alteration on the leaching behavior of B during water-rock interaction is also unknown. Nevertheless, despite these concerns, the data clearly show that the acid-sulfate fluids from NS9 react with the least altered (freshest) crust and those from DESMOS with the most intensely altered crust, which is in agreement with the temporal observations of volcanic activity in the eastern Manus Basin.

6. Summary and Conclusions

The formation of acid-sulfate fluids from the Manus Basin and the controls on the fluid chemistry have been investigated from the perspective of Li, B, Mg, and Sr isotopes and concentrations. Mg isotope ratios show that the high Mg concentrations in the acid-sulfate fluids from the Manus Basin cannot be explained by dissolution of Mg-bearing minerals. Instead, Mg appears to be seawater derived, since the Mg isotope ratios of all acid-sulfate fluids resemble those of seawater, which confirms the hypotheses that acid-sulfate fluids form in principal through direct injection of magmatic volatiles into unmodified seawater.

Sr isotope ratios deviating from seawater do, however, suggest that all acid-sulfate fluids are influenced by interaction with the basement. However, due to low reaction temperatures, Sr is not efficiently extracted from the basement, and as a consequence, the Sr isotope ratios in acid-sulfate fluids do not accurately reflect the extent of water-rock interaction. Further, Sr is influenced by precipitation and dissolution of anhydrite, making its interpretation even more challenging. Li, in contrast, is efficiently leached from the basement at acid-sulfate conditions, leading to a progressing depletion of Li in the volcanic rocks and an increase in δ^7Li during acid-sulfate alteration. Li concentrations and δ^7Li values of acid-sulfate fluids, thus, do not only record w/r ratios during water-rock interaction, but they also appear to be a tracer for basement alteration. Applying this to the acid-sulfate fluids from the Manus Basin, the δ^7Li values of EMVZ acid-sulfate fluids at DESMOS likely reflect a lack of recent volcanic activity and hence a lack of fresh near-surface volcanic material. In contrast, δ^7Li in the acid-sulfate fluids from North Su support a heterogeneously altered basement and supply of fresh volcanic material, consistent with the observed cryptodome eruption (2006–2011).

Since B is less affected by the basement alteration at acid-sulfate conditions than is Li, the combination of B and Li isotope ratios offers the potential to trace changing w/r ratios during water-rock interaction, basement alteration extents, and compositional heterogeneities in the basement. Nevertheless, to further test the veracity of combining B and Li concentrations and isotope ratios to trace basement alteration in these acidic environments, additional studies on acid-sulfate fluids from other settings with acid-sulfate fluids would be beneficial.

Acknowledgments
The authors would like to thank the crew of the R/V *Melville* and R/V *Sonne* as well as the technical groups of ROV *Jason II* and ROV *MARUM-QUEST*. This study was part of MARUM project GB4 and was funded by the DFG-Research Centre/Cluster of Excellence "The Ocean in the Earth System" at MARUM—Centre for Environmental Sciences, University of Bremen (EXC309/FZT15) and was supported from the German Research Foundation (DFG) Major Research Instrumentation Program (INST 144/308-1). We would also like to thank Dionysis Foustoukos and an anonymous reviewer for the thorough reviews, which improved the manuscript a lot. The data reported in this paper are archived in Pangaea (https://doi.pangaea.de/10.1594/PANGAEA.908303).

References

Albarède, F., Michard, A., Minster, J. F., & Michard, G. (1981). $^{87}Sr/^{86}Sr$ ratios in hydrothermal waters and deposits from the East Pacific Rise at 21°N. *Earth and Planetary Science Letters*, *55*, 229–236.

Araoka, D., Nishio, Y., Gamo, T., Yamaoka, K., & Kawahata, H. (2016). Lithium isotopic systematics of submarine vent fluids from arc and back-arc hydrothermal systems in the western Pacific. *Geochemistry, Geophysics, Geosystems*, *17*, 3835–3853. https://doi.org/10.1002/2016GC006355

Bach, W., Dubilier, N., Borowski, C., Breuer, C., Brunner, B., Franke, P., et al. (2011). Cruise Report for SONNE cruise SO 216—BAMBUS, Back-Arc Manus Basin Underwater Solfataras. Universität Bremen (https://elib.suub.uni-bremen.de/edocs/00102250-1.pdf).

Beier, C., Bach, W., Turner, S., Niedermeier, D., Woodhead, J., Erzinger, J., & Krumm, S. (2015). Origin of silicic magmas at spreading centres—An exampe from the South East Rift, Manus Basin. *Journal of Petrology*, *56*, 255–277.

Berndt, M. E., Seyfried, W. E., & Beck, J. W. (1988). Hydrothermal alteration processes at midocean ridges: Experimental and theoretical constraints from Ca and Sr exchange reactions and Sr isotopic ratios. *Journal of Geophysical Research*, *93*(B5), 4573–4583. https://doi.org/10.1029/JB093ib05p04573

Binns, R. A., Barriga, F. J. A. S., & Miller, D. J. (2007). In F. J. A. S. Barriga, R. A. Binns, D. J. Miller, & P. M. Herzig (Eds.), *Leg 193 synthesis: Anatomy of an active felsic-hosted hydrothermal system, eastern Manus Basin*, (pp. 1–71). Papua New Guinea (2007): Proceeding of the Ocean Drilling Program, Scientific Results 193. https://doi.org/10.2973/odp.proc.sr.193.201.2007

Butterfield, D. A. (1999). Deep ocean hydrothermal vents. In H. Sigurdsson (Ed.), *Encyclopedia of volcanoes*, (pp. 857–875). Cambridge, MA: Academic press.

Butterfield, D. A., Nakamura, K. I., Takano, B., Lilley, M. D., Lupton, J. E., Resing, J. A., & Roe, K. K. (2011). High SO_2 flux, sulfur accumulation, and gas fractionation at an erupting submarine volcano. *Geology*, *39*(9), 803–806.

Chan, L. H., Alt, J. C., & Teagle, D. A. (2002). Lithium and lithium isotope profiles through the upper oceanic crust: A study of seawater–basalt exchange at ODP Sites 504B and 896A. *Earth and Planetary Science Letters*, *201*(1), 187–201.

Chan, L. H., Edmond, J. M., Thompson, G., & Gillis, K. (1992). Lithium isotopic composition of submarine basalts: Implications for the lithium cycle in the oceans. *Earth and Planetary Science Letters*, *108*(1-3), 151–160.

Craddock, P. R., Bach, W., Seewald, J. S., Rouxel, O. J., Reeves, E., & Tivey, M. K. (2010). Rare earth element abundances in hydrothermal fluids from the Manus Basin, Papua New Guinea: Indicators of sub-seafloor hydrothermal processes in back-arc basins. *Geochimica et Cosmochimica Acta*, *74*, 5494–5513.

Davis, A. C., Bickle, M. J., & Teagle, D. A. H. (2003). Imbalance in the oceanic strontium budget. *Earth and Planetary Science Letters*, *211*, 173–187.

de Ronde, C. E. J., Massoth, G. J., Butterfield, D. A., Christenson, B. W., Ishibashi, J., Ditchburn, R. G., et al. (2011). Submarine hydrothermal activity and gold-rich mineralization at Brothers Volcano, Kermadec Arc, New Zealand. *Mineralium Deposita*, *46*(5-6), 541–584. https://doi.org/10.1007/s00126-011-0345-8

Flesh, G. D., Anderson, A. R., & Svec, H. J. (1973). A secondary isotopic standard for $^{7}Li/^{6}Li$ determination. *International Journal of Mass Spectrometry and Ion Physics*, *12*, 265–272.

Foster, G. L., Pogge von Strandmann, P. A. E., & Rae, J. W. B. (2010). Boron and magnesium isotopic composition of seawater. *Geochemistry, Geophysics, Geosystems*, *11*, Q08015. https://doi.org/10.1029/2010GC003201

Gamo, T., Okamura, K., Charlou, J. L., Urabe, T., Auzende, J. M., Ishibashi, J., et al. (1997). Acidic and sulfate-rich hydrothermal fluids from the Manus back-arc basin, Papua New Guinea. *Geology*, *25*(2), 139–142. https://doi.org/10.1130/0091-7613(1997)025<0139:AASRHF>2.3.CO;2

Gao, Y., & Casey, J. F. (2011). Lithium isotope composition of ultramafic geological reference materials: JP-1 and DTS-2. *Geostandards and Geoanalytical Research*, *36*, 75–81.

Garbe-Schönberg, D., Koschinsky, A., Ratmeyer, V., Jähmlich, H., & Westernströer, U. (2006). KIPS—A new multiport valve-based all-Teflon fluid sampling system for ROVs. In Geophys. Res. Abstr., 8,p. 07032.

Gena, K., Mizuta, T., Ishiyama, D., & Urabe, T. (2001). Acid-sulfate type alteration and mineralization in the Desmos caldera, Manus back-arc basin, Papua New Guinea. *Resource Geology*, *51*, 31–33.

Gena, K. R., Chiba, H., Mizuta, T., & Matsubaya, O. (2006). Hydrogen, oxygen and sulfur isotope studies of seafloor hydrothermal system at the Desmos caldera, Manus back-arc basin, Papua New Guinea: An analogue of terrestrial acid hot crater-lake. *Resource Geology*, *56*(2), 183–190.

Genske, F. S., Turner, S. P., Beier, C., Chu, M.-F., Tonarini, S., Pearson, N. J., & Haase, K. M. (2014). Lithium and boron isotope systematics in lavas from the Azores islands reveal crustal assimilation. *Chemical Geology*, *373*, 27–36.

Hansen, C. T., Meixner, A., Kasemann, S. A., & Bach, W. (2017). New insight on Li and B isotope fractionation during serpentinization derived from batch reaction investigations. *Geochimica et Cosmochimica Acta*, *217*, 51–79.

Hrischeva, E., Scott, S. D., & Weston, R. (2007). Metalliferous sediments associated with presently forming volcanogenic massive sulfides: The SuSu Knolls hydrothermal field, eastern Manus Basin, Papua New Guinea. *Economic Geology*, *102*(1), 55–73.

Huang, J., Ke, S., Gao, Y., Xiao, Y., & Li, S. (2015). Magnesium isotopic compositions of altered oceanic basalts and gabbros from IODP site 1256 at the East Pacific Rise. *Lithos*, *231*, 53–61.

Huang, K.-F., You, C.-F., Liu, Y.-H., Wang, R.-M., Lin, P.-Y., & Chung, C.-H. (2010). Low memory, small sample size, accurate and high-precision determinations of lithium isotopic ratios in natural materials by MC-ICP-MS. *Journal of Analytical Atomic Spectrometry*, *25*, 1019–1024.

Huang, K.-J., Teng, F.-Z., Plank, T., Staudigel, H., Hu, Y., & Bao, Z.-Y. (2018). Magnesium isotopic composition of altered oceanic crust and the global Mg cycle. *Geochimica et Cosmochimica Acta*, *238*, 357–373.

James, R. H., Allen, D. E., & Seyfried, W. E. Jr. (2003). An experimental study of alteration of oceanic crust and terrigenous sediments at moderate temperatures (51 to 350 °C): Insights as to chemical processes in near-shore ridge-flank hydrothermal systems. *Geochimica et Cosmochimica Acta*, *67*(4), 681–691.

Kamenetsky, V. S., Binns, R. A., Gemmell, J. B., Crawford, A. J., Mernagh, T. P., Maas, R., & Steele, D. (2001). Parental basaltic melts and fluids in eastern Manus backarcBasin: implications for hydrothermal mineralisation. *Earth and Planetary Science Letters*, *184*(3-4), 685–702.

Lackschewitz, K. S., Devey, C. W., Stoffers, P., Botz, R., Eisenhauer, A., Kummetz, M., et al. (2004). Mineralogical, geochemical and isotopic characteristics of hydrothermal alteration processes in the active, submarine, felsic-hosted PACMANUS field, Manus Basin, Papua New Guinea. *Geochimica et Cosmochimica Acta*, *68*(21), 4405–4427. https://doi.org/10.1016/j.gca.2004.04.016

Lee, S. M., & Ruellan, E. (2006). Tectonic and magmatic evolution of the Bismarck Sea, Papua New Guinea: Review and new synthesis. In D. M. Christie, C. R. Fisher, S.-M. Lee, & S. Givens (Eds.), *In Back-arc spreading systems: Geological, biological, chemical, and physical interactions, vol. 166*, (pp. 263–286). Washington DC: AGU Monograph. American Geophysical Union.

Lupton, J., Butterfield, D., Lilley, M., Evans, L., Nakamura, K. I., Chadwick, W. Jr., et al. (2006). Submarine venting of liquid carbon dioxide on a Mariana Arc volcano. *Geochemistry, Geophysics, Geosystems*, *7*, Q08007. https://doi.org/10.1029/2005GC001152

Magenheim, A. J., Spivack, A. J., Alt, J. C., Bayhurst, G., Chan, L. H., Zuleger, E., & Gieskes, J. M. (1995). Borehole fluid chemistry in hole 504B, leg 137: Formation water or in-situ reaction? *Proceeding of the Ocean Drilling Program, Scientific Results*, *137*(140), 141–152.

Millot, R., Scaillet, B., & Sanjuan, B. (2010). Lithium isotopes in island arc geothermal systems: Guadeloupe, Martinique (French West Indies) and experimental approach. *Geochimica et Cosmochimica Acta*, *74*, 1852–1871.

Moriguti, T., & Nakamura, E. (1998). High-yield lithium separation and the precise isotopic analysis for natural rock and aqueous samples. *Chemical Geology*, *145*(1-2), 91–104.

Park, S. H., Lee, S.-M., Kamenov, G. D., Kwon, S.-T., & Lee, K.-Y. (2010). Tracing the origin of subduction components beneath the South East rift in the Manus Basin, Papua New Guinea. *Chemical Geology*, *269*, 339–349.

Paulick, H., & Bach, W. (2006). Phyllosilicate alteration mineral assemblages in the active subsea-floor Pacmanus hydrothermal system, Papua New Guinea, ODP Leg 193. *Economic Geology*, *101*(3), 633–650.

Pearce, J. A., & Stern, R. J. (2006). Origin of back-arc basin magmas: trace element and isotope perspectives. In D. M. Christie, C. R. Fisher, S.-M. Lee, & S. Givens (Eds.), *Back-arc spreading systems: Geological, biological, chemical, and physical interactions, vol. 166*, (pp. 63–86). Washington DC: AGU Monograph. American Geophysical Union.

Pin, C., & Bassin, C. (1992). Evaluation of a-specific extraction chromatographic method for isotopic analysis in geological materials. *Analytica Chimica Acta*, *269*(2), 249–255.

Pistiner, J. S., & Henderson, G. M. (2003). Lithium-isotope fractionation during continental weathering processes. *Earth and Planetary Science Letters*, *214*(1-2), 327–339.

Pogge von Strandmann, P. A. E., Burton, K. W., James, R. H., van Calsteren, P., & Gislason, S. R. (2010). Assessing the role of climate on uranium and lithium isotope behaviour in rivers draining a basaltic terrain. *Chemical Geology*, *270*(1-4), 227–239.

Pogge von Strandmann, P. A. E. P., Elliott, T., Marschall, H. R., Coath, C., Lai, Y. J., Jeffcoate, A. B., & Ionov, D. A. (2011). Variations of Li and Mg isotope ratios in bulk chondrites and mantle xenoliths. *Geochimica et Cosmochimica Acta*, *75*(18), 5247–5268.

Pogge von Strandmann, P. A. E., James, R. H., van Calsteren, P., Gíslason, S. R., & Burton, K. W. (2008). Lithium, magnesium and uranium isotope behaviour in the estuarine environment of basaltic islands. *Earth and Planetary Science Letters*, *274*(3-4), 462–471. https://doi.org/10.1016/j.epsl.2008.07.041

Reeves, E. P., Seewald, J. S., Saccocia, P., Bach, W., Craddock, P. R., Shanks, W. C., et al. (2011). Geochemistry of hydrothermal fluids from the PACMANUS, Northeast Pual and Vienna Woods hydrothermal fields, Manus Basin, Papua New Guinea. *Geochimica et Cosmochimica Acta*, *75*(4), 1088–1123. https://doi.org/10.1016/j.gca.2010.11.008

Reeves, E. P., Thal, J., Schaen, A., Ono, S., Seewald, J., & Bach, W. (2015). Temporal evolution of magmatic-hydrothermal systems in the Manus Basin, Papua New Guinea: Insights from vent fluid chemistry and bathymetric observations (Invited). AGU Fall Meeting, abstract OS42A-05, San Francisco.

Resing, J. A., Lebon, G., Baker, E. T., Lupton, J. E., Embley, R. W., Massoth, G. J., & De Ronde, C. E. J. (2007). Venting of acid-sulphate fluids in a high-sulfidation setting at NW Rota-1 submarine volcano on the Mariana Arc. *Economic Geology*, *102*(6), 1047–1061.

Seewald, J. S., Doherty, K. W., Hammar, T. R., & Liberatore, S. P. (2002). A new gas-tight isobaric sampler for hydrothermal fluids. *Deep Sea Research Part I: Oceanographic Research Papers*, *49*(1), 189–196.

Seewald, J. S., Reeves, E. P., Bach, W., Saccocia, P. J., Craddock, P. R., Shanks, W. C. III, et al. (2015). Submarine venting of magmatic volatiles in the eastern Manus Basin, Papua New Guinea. *Geochimica et Cosmochimica Acta*, *163*, 179–199.

Seewald, J. S., Reeves, E. P., Bach, W., Saccocia, P. J., Craddock, P. R., Walsh, E., et al. (2019). Geochemistry of hot-springs at the SuSu Knolls hydrothermal field, eastern Manus Basin: Advanced argillic alteration and vent fluid acidity. *Geochimica et Cosmochimica Acta*, *255*, 25–48. https://doi.org/10.1016/j.gca.2019.03.034

Seyfried, W. E. (1987). Experimental and theoretical constraints on hydrothermal alteration processes at mid-ocean ridges. *Annual Review of Earth and Planetary Sciences*, *15*, 317–335.

Seyfried, W. E., Janecky, D. R., & Mottl, M. J. (1984). Alteration of the ocean crust: Implications for geochemical cycles of lithium and boron. *Geochimica et Cosmochimica Acta*, *48*(3), 557–569.

Sinton, J. M., Ford, L. L., Chappell, B., & McCulloch, M. T. (2003). Magma genesis and mantle heterogeneity in the Manus back-arc basin, Papua New Guinea. *Journal of Petrology*, *44*(1), 159–195.

Strelow, F. W., Rethemeyer, R., & Bothma, C. J. C. (1965). Ion exchange selectivity scales for cations in nitric acid and sulfuric acid media with a sulfonated polystyrene resin. *Analytical Chemistry*, *37*(1), 106–111.

Strelow, F. W. E. (1960). An ion exchange selectivity scale of cations based on equilibrium distribution coefficients. *Analytical Chemistry*, *32*(9), 1185–1188.

Taylor, B., Crook, K., & Sinton, J. (1994). Extensional transform zones and oblique spreading centers. *Journal of Geophysical Research*, *99*(B10), 19707–19718.

Teng, F.-Z., Hu, Y., & Chauvel, C. (2016). Magnesium isotope geochemistry in arc volcanism. *Proceedings of the National Academy of Sciences*, *113*(26), 7082–7087.

Teng, F.-Z., Li, W.-Y., Ke, S., Marty, B., Dauphas, N., Huang, S., et al. (2010). Magnesium isotopic composition of the Earth and chondrites. *Geochimica et Cosmochimica Acta*, *74*(14), 4150–4166. https://doi.org/10.1016/j.gca.2010.04.019

Thal, J., Tivey, M., Yoerger, D. R., & Bach, W. (2016). Subaqueous cryptodome eruption, hydrothermal activity and related seafloor morphologies on the andesitic North Su volcano. *Journal of Volcanology and Geothermal Research*, *323*, 80–96.

Tivey, M., Bach, W., Seewald, J., Tivey, M. K., Vanko, D. A., & the Shipboard Science (2006). Cruise Report for R/V *Melville* cruise MGLN06MV—Hydrothermal systems in the eastern Manus Basin: Fluid chemistry and magnetic structure as guides to subseafloor processes. Woods Hole Oceanographic Institution (available upon request to authors).

Verney-Carron, A., Vigier, N., Millot, R., & Hardarson, B. S. (2015). Lithium isotopes in hydrothermally altered basalts from Hengill (SW Iceland). *Earth and Planetary Science Letters*, *41*, 62–71.

Voigt, M., Pearce, C. R., Baldermann, A., & Oelkers, E. H. (2018). Stable and radiogenic strontium isotope fractionation during hydrothermal seawater-basalt interaction. *Geochimica et Cosmochimica Acta*, *240*, 131–151.

Wilckens, F. K., Reeves, E. P., Bach, W., Meixner, A., Seewald, J. S., & Kasemann, S. A. (2018). The influence of magmatic fluids and phase separation on B systematics in submarine hydrothermal vent fluids from back-arc basins. *Geochimica et Cosmochimica Acta*, *232*, 140–162.

Yamaoka, K., Hong, E., Ishikawa, T., Gamo, T., & Kawahata, H. (2015). Boron isotope geochemistry of vent fluids from arc/back-arc seafloor hydrothermal systems in the western Pacific. *Chemical Geology*, *392*, 9–18.

Yamaoka, K., Ishikawa, T., Matsubaya, O., Ishiyama, D., Nagaishi, K., Hiroyasu, Y., et al. (2012). Boron and oxygen isotope systematics for a complete section of oceanic crustal rocks in the Oman ophiolite. *Geochimica et Cosmochimica Acta*, *84*, 543–559.

Young, E. D., & Galy, A. (2004). The isotope geochemistry and cosmochemistry of magnesium. *Reviews in Mineralogy and Geochemistry*, *55*(1), 197–230.